
Online continual learning with no task boundaries

Rahaf Aljundi^{1,2} Min Lin² Baptiste Goujaud² Yoshua Bengio²

Abstract

Continual learning is the ability of an agent to learn online with a non-stationary and never-ending stream of data. A key component for such never-ending learning process is to overcome the catastrophic forgetting of previously seen data, a problem that neural networks are well known to suffer from. The solutions developed so far often relax the problem of continual learning to the easier task-incremental setting, where the stream of data is divided into tasks with clear boundaries. In this paper, we break the limits and move to the more challenging online setting where we assume no information of tasks in the data stream. We start from the idea that each learning step should not increase the losses of the previously learned examples through constraining the optimization process. This means that the number of constraints grows linearly with the number of examples, which is a serious limitation. We develop a solution to select a fixed number of constraints that we use to approximate the feasible region defined by the original constraints. We compare our approach against the methods that rely on task boundaries to select a fixed set of examples, and show comparable or even better results, especially when the boundaries are blurry or when the data distributions are imbalanced.

1. Introduction

The most general form of the continual learning problem can be described as the learning problem where data are streamed online and there is no independent and identically distributed (i.i.d.) assumption on the distribution of the streamed data. Systems designed to solve the continual learning problem should be featured with the following desiderata:

Online learning. Learning needs to take place online as the data arrive.

¹KU Leuven ²Mila. Correspondence to: Rahaf Aljundi <rahaf.aljundi@gmail.com>.

Bounded system size. There is a budget limit on the computation and storage resources that the algorithm can use to perform online learning.

Forward and backward transfer. The knowledge being learned should be able to generalize to the data observed in the future. It should also generalize and improve performance on previous data if these were to appear again.

Prevention of catastrophic forgetting. Catastrophic forgetting is the tendency of neural networks trained online to abruptly forget information on old training data when updated with the new data, in the case these new data and the old ones come from different distributions. Catastrophic forgetting is the major obstacle to continual learning.

No requirement of task boundaries. Either there is no explicit notion of tasks, or the information on task boundaries is unknown for the data stream.

While all continual learning methods try to overcome “catastrophic forgetting”, almost all of them have different levels of relaxations on the above desiderata. Of all desiderata, “online learning” is the most commonly violated due to the difficulty of strict per-example incremental learning. Although the per-example incremental setting is used in some early works (Robins, 1995), it is applied on very small toy datasets of only 10 incremental learning steps. More recent works, however, usually learn with hundreds of thousands of examples (Li & Hoiem, 2016; Rusu et al., 2016). Therefore, they adopt a milder task incremental assumption: the data are streamed one task at a time, with different distributions for each task, while keeping the i.i.d. assumption and performing offline training within each task learning phase. Methods developed using this setting often require the availability of task boundaries during training, and even during testing for some methods. Availability of task boundaries overly reduces the difficulty of the continual learning problem. On the one hand, one can argue that under this setting we could train one model for each task to avoid catastrophic forgetting. On the other hand, this is also in contradiction with the fact that the task boundaries are often not available in real-world tasks. In fact, the task boundaries could be blurry or there could even be no notion of tasks. For example, in reinforcement learning, there could be a gradual change of scenes as the agent takes actions, which will not be notified to the agent through extra information

such as the task id.

In this work, we aim to move closer to the more strict online learning setting, where there is no information about task boundaries to depend on and data are streamed in an online, non-stationary, manner. We start by formulating continual learning as a constrained optimization problem where the losses of the previously learned examples should not increase. We develop an algorithm to select a fixed number of the previous examples to provide the constraints, with the goal to have the feasible region defined by these selected constraints approximates the feasible region of the original problem with all the past examples. Our contributions are as follows:

1. We propose an algorithm that performs constraint selection without the knowledge of the task boundaries, and we formalize it as a solid angle minimization problem.
2. We propose a surrogate objective for it and empirically verify that the surrogate objective aligns with the goal of solid angle minimization.
3. We perform experiments on continual learning benchmarks and show that our method is on par with, or better than, the previous methods.

In the next section, we review three major families of continual learning methods in the light of the above desiderata, with special emphasis on their requirements of task boundaries.

2. Related Work

Current continual learning methods can be categorized into three major families based on how the information of previous data are stored and used. We describe each of them below. The *prior-focused* approach converts this information into the distribution of the parameters of the model, which is then used as the prior distribution when learning new data. The *replay-based* approach stores the information in the example space either directly in a replay buffer, or compressed in a generative model. When learning new data, old examples are reproduced from the replay buffer or generative model, which is used for rehearsal/retraining or used as constraints for the current learning. We call this category replay-based instead of rehearsal-based since conventionally rehearsal implies retraining, yet the old examples could also be used to provide constraints (Lopez-Paz et al., 2017). We term the last major family as *parameter isolation*, which uses isolated parameters for different tasks to prevent interference. Dynamic architectures that freeze/grow the network belong to this family. However, it is also possible to isolate parameters without changing the architecture (French, 1994; Mallya & Lazebnik, 2018).

2.1. Prior-focused methods

Elastic weight consolidation (EWC) (Kirkpatrick et al., 2017), Synaptic Intelligence (SI) (Zenke et al., 2017) and Variational Continual Learning (VCL) (Nguyen et al., 2017) are representative methods of the prior-focused family. For prior-focused methods, the dimension of the parameter space is usually too high to model general distributions on it. As an approximation, it is usually assumed that each parameter has an independent Gaussian distribution. Therefore these methods only require one extra scalar for each synapse to store the importance score (e.g. inverse of Gaussian variance). It seems that the requirement of task boundaries can be removed from the prior-focused methods by treating every batch/example as a unique task. In fact, there is recent work that brings the prior-focused method into the online setting (Aljundi et al., 2018a). However, prior-focused methods use a penalty term to regularize the parameters rather than a hard constraint. The parameter gradually drifts away from the feasible regions of previous tasks, especially when there is a long chain of tasks and when the tasks resemble each other (Farquhar & Gal, 2018).

Therefore, although the prior-focused methods enjoy the beauty of the Bayesian framework, practically their performance is usually unsatisfying. It is often necessary to hybridize the prior-focused approach with the replay-based methods for better results (Nguyen et al., 2017; Farquhar & Gal, 2018), i.e. keep a core-set of the previous training examples and perform rehearsal on it.

2.2. Replay-based methods

The replay-based approach stores the previous examples directly in the example space. Although storage of the original examples in memory for rehearsal dates back to 1990s (Robins, 1995), to date it is still a rule of thumb to overcome catastrophic forgetting in practical problems. For example, experience replay is widely used in reinforcement learning where the data distributions are usually non-stationary and prone to catastrophic forgetting (Lin, 1993; Mnih et al., 2013). Recent works in this family include iCaRL (Rebuffi et al., 2017) and GEM (Lopez-Paz et al., 2017), both of which allocate memory to store a core-set of examples from each task. These methods still require task boundaries in order to divide the storage resource evenly to each task. GEM has an extra dependence on task boundaries because it adds to the objective one constraint for each task.

Recent success on generative adversarial networks (GAN) (Goodfellow et al., 2014) has also opened up the possibility to store and replay the previous examples with a GAN (Shin et al., 2017). However, this also adds the complexity that we need to train the GAN continually, which also depends on availability of task boundaries to keep balanced examples and avoid the mode collapse problem (Mariani et al., 2018).

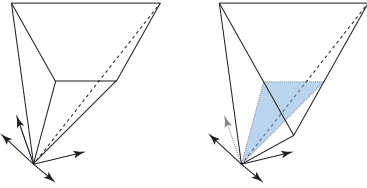


Figure 1. Feasible region (polyhedral cone) before and after constraint selection. The selected constraints (excluding the blue one) are chosen to best approximate the original feasible region.

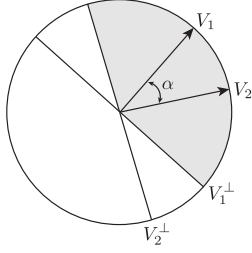


Figure 2. Relation between angle formed by two vectors (α) and the associated feasible set (grey region)

2.3. Parameter isolation methods

Methods in this family attempt to remove the interference between examples by using different sets of parameters for different examples. One subset of this family requires dynamically changing the neural network architecture. It prevents forgetting by freezing part of the weights while preserving the ability to learn new information by growing the network (Rusu et al., 2016; Xu & Zhu, 2018). It is also possible to isolate the parameters used for each task with a pre-fixed architecture (Mallya & Lazebnik, 2018). Both of the above strategies explicitly associate neurons with different tasks, with the consequence that task boundaries are mandatory during both training and testing so as to decide which neurons should be activated. Due to the dependency on task boundaries during test, this family of methods tilts more towards multi-task learning than continual learning. It is worth noting that part of the experiments in previous works that use multiple output heads for different tasks can also be seen as parameter isolation (Li & Hoiem, 2016; Nguyen et al., 2017). Hence, it is not recommended to use multi-head output for continual learning, because it adds the dependency on task boundaries during test.

3. Continual learning as constrained optimization

We consider the supervised learning problem with an online stream of data where one or a few pairs of examples (x, y)

are received at a time. The data stream is non-stationary with no assumption on the distribution such as the i.i.d. hypothesis. Our goal is to optimize the loss on the current example(s) without increasing the losses on the previously learned examples.

3.1. Problem formulation

We formulate our goal as the following constrained optimization problem. Without loss of generality, we assume the examples are observed one at a time.

$$\theta^t = \operatorname{argmin}_{\theta} \ell(f(x_t; \theta), y_t) \quad (1)$$

$$\text{s.t. } \ell(f(x_i; \theta), y_i) \leq \ell(f(x_i; \theta^{t-1}), y_i); \forall i \in [0 \dots t-1]$$

$f(\cdot; \theta)$ is a model parameterized by θ and ℓ is the loss function. t is the index of the current example and i indexes the previous examples.

As suggested by (Lopez-Paz et al., 2017), the original constraints can be rephrased to the constraints in the gradient space:

$$\langle g, g_i \rangle = \left\langle \frac{\partial \ell(f(x_t; \theta), y_t)}{\partial \theta}, \frac{\partial \ell(f(x_i; \theta), y_i)}{\partial \theta} \right\rangle \geq 0; \quad (2)$$

However, the number of constraints in the above optimization problem increases linearly with the number of previously learned examples. The required computation and storage resource for an exact solution of the above problem will increase indefinitely with time. It is thus more desirable to solve the above problem approximately with a fixed computation and storage budget.

3.2. Gradient Episodic Memory

GEM proposes an approximation of 2 by using an *episodic memory* \mathcal{M} limited to M memory slots. The constraints are only active for $(x_i, y_i) \in \mathcal{M}$. It assumes access to task boundaries and an i.i.d. distribution within each task episode. Consequently, the memory budget can be divided evenly among the tasks. i.e. $m = M/T$ slots is allocated for each task, where T is the number of tasks. The last m examples from each task are kept in the memory.

There are a few limitations of GEM that we think can be improved. 1. The requirement of task boundaries prevents it from being applied to a more general continual learning setting where there is no task id or even no notion of task. 2. The selection strategy within each task that simply keeps the last m examples is also very primitive. Given that our goal is to approximate the original optimization problem with a subset of the constraints, it would be more desirable to keep the subset that best captures the sufficient statistics of all previous data than keeping a random subset.

3.3. Constraint selection without task boundaries

With a budget of M memory locations, we aim to select M of the constraints so that the feasible region bounded by the selected constraints is close to the feasible region of the original problem. We first convert the original constraints in 2 to the corresponding feasible region:

$$C = \bigcap_{i \in [0..t-1]} \{g | \langle g, g_i \rangle \geq 0\} \quad (3)$$

Geometrically, C is the intersection of the half spaces described by $\langle g, g_i \rangle \geq 0$, which forms a polyhedral convex cone. The relaxed feasible region in our fixed budget approximation is:

$$\tilde{C} = \bigcap_{g_i \in \mathcal{M}} \{g | \langle g, g_i \rangle \geq 0\} \quad (4)$$

For best approximation of the original feasible region, we require \tilde{C} to be as close to C as possible. It is easy to see that $C \subset \tilde{C}$ because $\mathcal{M} \subset [g_0 .. g_{t-1}]$. We illustrate the relation between C and \tilde{C} in Figure 1.

On the left, C is represented while the blue hyperplane on the right corresponds to a constraint that has been removed. Therefore, \tilde{C} (on the right) is larger than C for the inclusion partial order. As we want \tilde{C} to be as close to C as possible, we actually want the "smallest" \tilde{C} , where "small" here remains to be defined, as the inclusion order is not a complete order. A good measure of the size of a convex cone is its solid angle defined as the intersection between the cone and the unit sphere. Therefore, solving 5 would achieve our goal.

$$\text{minimize}_{\mathcal{M}} \lambda_{d-1} \left(S_{d-1} \cap \bigcap_{g_i \in \mathcal{M}} \{g | \langle g, g_i \rangle \geq 0\} \right) \quad (5)$$

where d denotes the dimension of the space, S_{d-1} the unit sphere in this space, and λ_{d-1} the Lebesgue measure in dimension $d - 1$.

Note that, in practice, the number of constraints and thus the number of gradients is likely to be way smaller than the dimension of the gradient, which means that the feasible space can be seen as the Cartesian product between its own intersection with $\text{span}(\mathcal{M})$ and the orthogonal subspace of $\text{span}(\mathcal{M})$. That being said, we can actually reduce our interest to the size of the solid angle in the M -dimensional space $\text{span}(\mathcal{M})$, as in 6.

$$\text{minimize}_{\mathcal{M}} \lambda_{M-1} \left(S_{M-1}^{\text{span}(\mathcal{M})} \cap \bigcap_{g_i \in \mathcal{M}} \{g | \langle g, g_i \rangle \geq 0\} \right) \quad (6)$$

where $S_{M-1}^{\text{span}(\mathcal{M})}$ denotes the unit sphere in $\text{span}(\mathcal{M})$.

Note that even if the sub-spaces $\text{span}(\mathcal{M})$ are different from each other, they all have the same dimension as M , which is fixed, hence comparing their λ_M -measure makes sense.

However, this objective is hard to minimize since the formula of the solid angle is complex, as shown in (Ribando, 2006) and (Beck et al., 2009). Therefore, we propose, in the next section, a surrogate to this objective that is easier to deal with.

3.4. An empirical surrogate to feasible region minimization

Intuitively, to decrease the feasible set, one must increase the angles between each pair of gradients. Indeed, this can be verified in 2D with Figure 2.

If this is achieved, a good objective would be Eq.7. Again, in 2D, one can be convinced that this objective is exact.

$$\begin{aligned} & \text{minimize}_{\mathcal{M}} \sum_{i,j \in \mathcal{M}} \frac{\langle g_i, g_j \rangle}{\|g_i\| \|g_j\|} \\ & \text{s.t. } \mathcal{M} \subset [0..t-1]; |\mathcal{M}| = M \end{aligned} \quad (7)$$

However, in higher dimension, the relation is less clear. Nevertheless, it sounds reasonable thinking that a correlation should exist between 6 and 7. This is highlighted in Figure 3, which shows the relation between the solid angle and our criterion defined in 7, for spaces of different dimensions. Here the solid angle has been normalized so that the whole sphere has an angle of one, which implies that the feasible set has an angle that lives between 0 and $\frac{1}{2}$.

Indeed, we see in 3D that, even if the Pearson correlation coefficient is not exactly 1, it is still high. Here, it is about 0.991, while in 8D, it is about 0.963 and in 200D it is about 0.799, making this surrogate legit. Note that this statistic just conveys the linear dependency between the 2 variables, so this is just a lower bound of the best R^2 statistic that we could get by fitting the observed curve in 3 with a larger class of functions. For instance if we fit the log values with a linear function, we get a correlation value of 0.99 even in 200D. However, the Pearson test is good enough, as the p-value is much smaller than any computer precision, and this is the reason why we did it in first approximation even if the dependency look much more exponential as we can see in 3d.

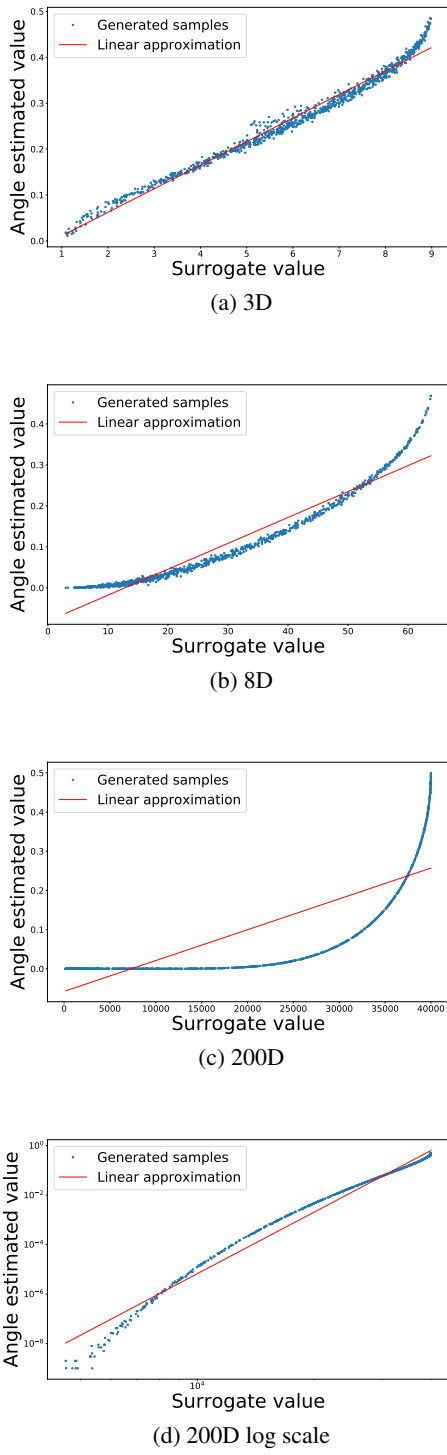


Figure 3. Correlation between solid angle and proposed surrogate in different dimensions

It is also worth noting that we only need monotonicity for the purpose of sample selection, so minimizing our surrogate would correspond to minimizing the solid angle.

3.5. Implementation Details

The strict implementation of the above idea implies performing a selection of constraints from the full history of examples at every iteration, which also becomes infeasible in practice. Instead, we keep a backup buffer \mathcal{M}_b with fixed capacity from which we select the active constraints \mathcal{M}_a . Also, examples in this backup buffer are selected online from the data stream with the same method that we use to select the active constraints. We also observe that the gradients do not change much within a local time window, which means that the active constraints will remain the same. Hence to avoid unnecessary re-selection of active constraints at every step, we keep track of how much the gradient directions differ from when they were estimated during previous constraint selection; we then redo the selection only when the difference exceeds a predefined threshold. The exact procedures are described in algorithm 1.

Projecting the gradient exactly into the feasible region is computationally very expensive. An usual work around for constrained optimization is to convert the constraints to a soft regularization loss. In our case, this is equivalent to performing rehearsal on the buffer. Although it is argued in (Lopez-Paz et al., 2017) that performing rehearsal on a limited set of examples could lead to overfitting, this could be alleviated since we have a better strategy at selecting the examples. Therefore, we also report results based on rehearsal as a cheaper alternative.

4. Experiments

This section serves to validate our approach and show its effectiveness at dealing with continual learning problems where task boundaries are not available.

4.1. Datasets

In this paper, we use the following datasets that are created from the original MNIST and CIFAR-10 datasets.

Disjoint MNIST. In disjoint MNIST, the dataset is divided into 5 tasks based on the labels. Each task contains only examples with two labels, without overlapping labels between tasks. We use 1000 examples per task for training and report results on all test examples. These tasks are sequentially ordered into a stream of tasks in the same way as described in (Zenke et al., 2017).

Algorithm 1 Online continual learning with no task boundaries

```

1: Input:  $\tau, \alpha, n, M_r, M_b, M_a, B$ 
2: function Constraints( $\mathcal{M}$ )
3:   for  $x_i, y_i$  in  $\mathcal{M}$  do
4:      $C_i \leftarrow \nabla_{\theta} \ell(f(x_i; \theta), y_i)$ 
5:      $C_i \leftarrow C_i / \|C_i\|$  {normalize the gradients}
6:   end for
7:   return  $C$ 
8: end function
9: function ConstrainedUpdate( $x, y, \mathcal{M}_a, \hat{C}$ )
10:  for iter in  $1 \dots n$  do
11:     $g \leftarrow \nabla_{\theta} \ell(f(x; \theta), y)$ 
12:     $C \leftarrow \text{Constraints}(\mathcal{M}_a)$ 
13:    if  $\hat{C}_i^T C_i < \tau$  for any  $i$  then
14:       $\mathcal{M}_a \leftarrow \text{SelectConstraints}(\mathcal{M}_b, M_a)$ 
15:       $C \leftarrow \text{Constraints}(\mathcal{M}_a), \hat{C} \leftarrow C$ 
16:    end if
17:     $g \leftarrow \text{project}(g, C)$ 
18:     $\theta = \theta - \alpha g$ 
19:  end for
20:  return  $\mathcal{M}_a, \hat{C}$ 
21: end function
22: function SelectConstraints( $\mathcal{M}, M$ )
23:    $\hat{\mathcal{M}} \leftarrow \underset{\hat{\mathcal{M}}}{\operatorname{argmin}} \sum_{i,j \in \hat{\mathcal{M}}} \frac{\langle g_i, g_j \rangle}{\|g_i\| \|g_j\|}$ 
24:   s.t.  $\hat{\mathcal{M}} \subset \mathcal{M}; |\hat{\mathcal{M}}| = M$ 
25:   return  $\hat{\mathcal{M}}$ 
26: end function
27: Initialize:  $\mathcal{M}_r, \mathcal{M}_b, \mathcal{M}_a, \hat{C} \leftarrow \text{Constraints}(\mathcal{M}_a)$ 
28: Receive:  $(x, y)$  {one or few consecutive examples}
29:  $\mathcal{M}_a, \hat{C} \leftarrow \text{ConstrainedUpdate}(x, y, \mathcal{M}_a, \hat{C})$ 
30:  $\mathcal{M}_r \leftarrow \mathcal{M}_r \cup \{(x, y)\}$ 
31: if len( $\mathcal{M}_r$ )  $> M_r$  then
32:    $\mathcal{B} \leftarrow \text{SelectConstraints}(\mathcal{M}_r, B)$ 
33:    $\mathcal{M}_r = \{\}$ 
34:    $\mathcal{M}_b \leftarrow \mathcal{M}_b \cup \mathcal{B}$ 
35:   if  $\mathcal{M}_b$  is full then
36:      $\mathcal{M}_b \leftarrow \text{SelectConstraints}(\mathcal{M}_b, M_b)$ 
37:      $\mathcal{M}_a \leftarrow \text{SelectConstraints}(\mathcal{M}_b, M_a)$ 
38:   end if
39: end if
```

Permuted MNIST. Besides disjoint MNIST, permuted MNIST is also a frequently used MNIST-based setting in previous works (Lopez-Paz et al., 2017; Kirkpatrick et al., 2017). In the case of permuted MNIST, we perform 10 unique permutations on the pixels of the MNIST images. The permutations result in 10 different tasks with same distributions of labels but different distributions of the input images. Following (Lopez-Paz et al., 2017), each of the task in permuted MNIST contains only 1000 training examples. The test set for this dataset is the union of the MNIST test

set with all different permutations.

Disjoint CIFAR-10. For CIFAR-10, we consider the same setting as disjoint MNIST. Namely, the dataset is split into 5 tasks according to the labels, with two labels in each task. Similar to disjoint MNIST, we use a total of 5000 training examples with 1000 examples per task.

4.2. Models

We use different models for MNIST and CIFAR-10. For MNIST we use a two-layer neural network with 100 neurons each. For CIFAR-10 we use ResNet18. Those architectures were used in (Lopez-Paz et al., 2017). Note that we employ a shared head in the incremental classification experiments, which is much more challenging than the multi-head used in (Lopez-Paz et al., 2017).

4.3. Compared Methods

For all the experiments, we consider the following baselines:

Single is a model trained online on the stream of data without any mechanism to prevent forgetting.

i.i.d. online is the Single baseline trained on an i.i.d. stream of the data.

i.i.d. offline is a model trained offline for multiple epochs with i.i.d. batches from all the training data.

We also compare against the following two closely related methods:

GEM (Lopez-Paz et al., 2017) stores a fixed amount of random examples per task and uses them to provide constraints when learning new examples.

iCaRL (Rebuffi et al., 2017) follows an incremental classification setting. It also stores a fixed number of examples per class but uses them to rehearse the network when learning new information.

For our method, we report both **Ours_Constrained** and **Ours_Rehearsal**. **Ours_Constrained** is the constraint based solution where the active constraints are selected and used during training to project the gradient of the seen examples onto the feasible region. **Ours_Rehearsal** is the cheaper alternative where at each iteration we select a random batch from \mathcal{M}_b and perform an extra parameter update on the random batch.

4.4. Performance under standard setup

In this part, we test our method directly on the task incremental datasets described in Section 4.1, with the exception that we ignore the information of task boundaries and treat them as any normal data stream. This places us at a disadvantage because the methods that we compare to utilize

the task boundaries as an extra information. In spite of this disadvantage, we show that our method performs similarly on these datasets.

Figure 4a shows the test accuracy on disjoint MNIST which is evaluated during the training procedure at an interval of 100 training examples. iCaRL, GEM and ours use a memory of 200 examples. For the i.i.d. baselines, we only show the achieved performance at the end of the training. For iCaRL, we only show the accuracy at the end of each task because iCaRL uses the selected exemplars for prediction that only happens at the end of each task. We observe that both variants of our method have a very similar learning curve to GEM except the very last iterations where the performance slightly drops.

Figure 4b compares our method with the baselines and GEM on the permuted MNIST dataset. Note that iCaRL is not included, as it is designed only for incremental classification. From the good performance of the Single baseline it is apparent that permuted MNIST has less interference between the different tasks. Our methods perform better than GEM and reach the performance of i.i.d online scenario.

Figure 4c shows the accuracy on the Disjoint CIFAR-10 evaluated during the training procedure at an interval of 100 training examples. It can be observed that accuracies of all the methods are low but this is justifiable if we look at the performance of the i.i.d online baseline, which is 0.29, using 5000 training examples. Because CIFAR-10 has more diverse data than MNIST, we can only get sensible results for all the methods at a minimal buffer of 600. This significantly increases the computation for gradient projection, therefore we only report results of Ours_Rehearsal. Ours_Rehearsal compares favorably to GEM and iCaRL, and it even achieves a better average test performance at the end of the sequence, which gets close to the i.i.d online. Note that our setting is much harder than iCaRL (Rebuffi et al., 2017), where data from each task is learned offline.

4.5. Performance under blurry task boundary

In this section, we demonstrate that our method is robust to the scenario where there are no clear task boundaries in the data stream, as we mentioned in introduction 1 that such situation can happen in practice. We start by blurring the task boundaries in the benchmarks. For each task in a dataset, we keep the majority of the examples while we randomly swap a small percentage of the examples with other tasks. A larger swap percentage corresponds to more blurry boundaries. A similar setting has been used in (Aljundi et al., 2018b). We make comparisons to the Single baseline and GEM. For GEM, the datasets are treated as if there is no random swap.

Figure 5 shows the results on the three datasets when the

Table 1. The effect of the buffer size. * denotes access to task identifiers.

Method \ Buffer Size	100	200	300	400
GEM*	0.78	0.85	0.87	0.88
iCaRL*	0.81	0.82	0.84	0.85
Ours Constrained	0.50	0.74	0.82	0.87
Ours Rehearsal	0.61	0.73	0.84	0.87

task boundaries are made blurry. We keep 90% of the data for each task, and introduce 10% of data from the other tasks. Our method is consistently better than GEM for all three datasets.

We understand that the comparison we conduct with GEM might not be fair, because GEM is not designed for blurry task boundaries. Nonetheless, this result shows the situation where the data stream is non-stationary, so there is no i.i.d. assumption to make conventional stochastic training works well; yet there are no clear task boundaries so that previous continual methods do not work either. Our method gives a reasonable learning curve under this situation that fills the gap.

4.6. Performance on i.i.d. data stream

As our method is designed to be agnostic to the distribution of the data stream, we study whether it could also improve over the naïve SGD training on the i.i.d. data streams. From the comparisons shown in Figure 6, it can be seen that our method does improves over the SGD baseline for all three datasets. This is especially true at the early stage of the training.

4.7. Effect of buffer size

Here we aim at testing the effect of the buffer size on the achieved performance of the compared methods and ours. We test the buffer sizes of (100, 200, 300 and 400) on the disjoint MNIST benchmark. Table 1 reports the test accuracy at the end of the training stream. iCaRL seems to perform the best on a smaller buffer size with only 100 examples. However, it achieves less performance than both ours and GEM on the larger sizes. While it seems that both our variants lose performance on the smaller buffer sizes, we think this might be a special case of disjoint MNIST, as it can be seen in Figure 4a that with buffer size 200 the accuracy of our method only decreases at the last few iterations. Nevertheless, on both permuted MNIST and disjoint CIFAR-10 we achieve similar results to GEM when using small buffers. Also note that for our approach a memory of size 100 has examples representative of the new task while for GEM all of the examples in the memory are from the previous tasks.

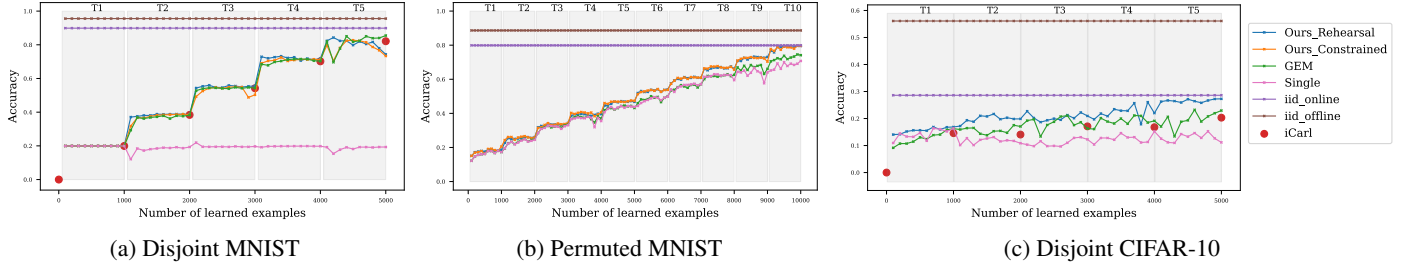


Figure 4. Test accuracy on three datasets with the standard setup

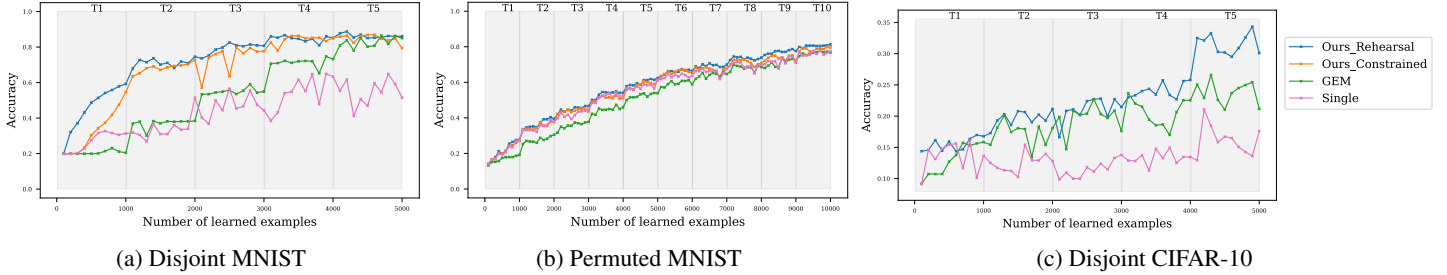


Figure 5. Test accuracy on three datasets with blurry boundaries throughout training

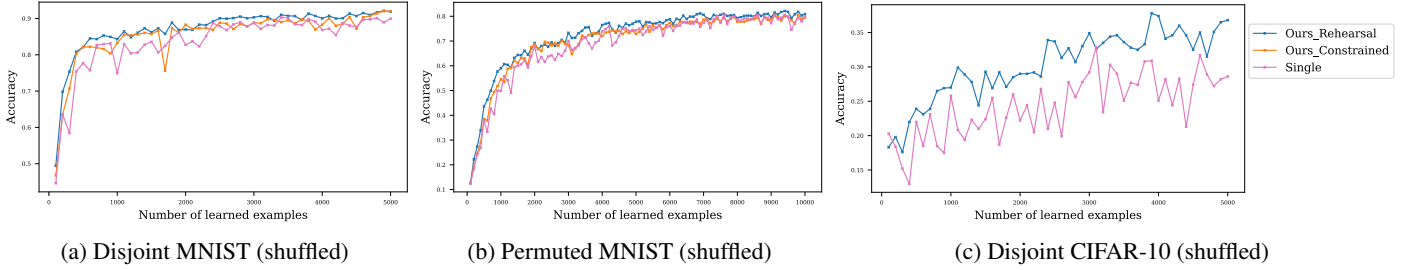


Figure 6. Test accuracy on the three datasets randomly shuffled to be i.i.d.

Table 2. Ours Rehearsal v.s. Rehearsal with reservoir sampling on imbalanced data stream. Accuracy on each task at the end of the training.

Method	T1	T2	T3	T4	T5	Overall
Reservoir Rehearsal	0.69	0.74	0.79	0.59	0.90	0.74
Ours Rehearsal	0.81	0.72	0.77	0.84	0.86	0.81

4.8. Comparison with reservoir sampling

Reservoir sampling (Vitter, 1985) is a simple replacement strategy to fill the memory buffer when the task boundaries are unknown based on the underlying assumption that the overall data stream is i.i.d distributed. It would work well when each of the tasks has a similar number of examples. However, it could lose the information on the under-represented tasks if some of the tasks have significantly fewer examples than the others. Our strategy has no assumption on the data stream distribution, hence it could be less

affected by imbalanced data, which is often encountered in practice. We test this effect on the disjoint MNIST dataset. We modify the data stream in which the second and third tasks have 4 times more examples than the rest. We also compare our method with reservoir sampling on this imbalanced dataset. We use the rehearsal variant for both our method and reservoir sampling. Table 2 reports the accuracy on each task achieved at the end of the training by the two methods. It can be seen that our constraint selection is less sensitive to the imbalanced data stream. It outperforms

reservoir sampling by a margin of 12% and 25% in accuracy on the first and third tasks, which are under-represented, while achieving similar performance on the other tasks.

5. Conclusion and future work

In this paper, we prove that in the online continual learning setting we can smartly select a finite number of data to be representative of all previously seen data without knowing task boundaries. We still perform as well as algorithms that use the knowledge of task boundaries to select the representative examples. Moreover, our selection strategy gives us advantage under the settings where the task boundaries are blurry or data are imbalanced.

In section 3.3, we point out the fact that we have to introduce a new measure to compare the cones, as the inclusion order is not complete. Using solid angle as the measure is one choice we make. However, another proposal could help in dealing with other concerns, an example will follow. Noticing that a candidate cone \tilde{C} can lead to possible far away point to original cone C while having a small solid angle, one might for instance be interested in minimizing the worst distance between any point of $\tilde{C} \cap S_{d-1}$ and its projection onto C . This might be a promising direction for future work.

References

- Aljundi, R., Kelchtermans, K., and Tuytelaars, T. Task-free continual learning. *arXiv preprint arXiv:1812.03596*, 2018a.
- Aljundi, R., Rohrbach, M., and Tuytelaars, T. Selfless sequential learning. *arXiv preprint arXiv:1806.05421*, 2018b.
- Beck, M., Robins, S., and Sam, S. V. Positivity theorems for solid-angle polynomials. *arXiv preprint arXiv:0906.4031*, 2009.
- Farquhar, S. and Gal, Y. Towards robust evaluations of continual learning. *arXiv preprint arXiv:1805.09733*, 2018.
- French, R. M. Dynamically constraining connectionist networks to produce distributed, orthogonal representations to reduce catastrophic interference. *network*, 1111:00001, 1994.
- Goodfellow, I., Pouget-Abadie, J., Mirza, M., Xu, B., Warde-Farley, D., Ozair, S., Courville, A., and Bengio, Y. Generative adversarial nets. In *Advances in neural information processing systems*, pp. 2672–2680, 2014.
- Kirkpatrick, J., Pascanu, R., Rabinowitz, N., Veness, J., Desjardins, G., Rusu, A. A., Milan, K., Quan, J., Ramalho, T., Grabska-Barwinska, A., et al. Overcoming catastrophic forgetting in neural networks. *Proceedings of the national academy of sciences*, pp. 201611835, 2017.
- Li, Z. and Hoiem, D. Learning without forgetting. *arXiv preprint arXiv:1606.09282*, 2016.
- Lin, L.-J. Reinforcement learning for robots using neural networks. Technical report, Carnegie-Mellon Univ Pittsburgh PA School of Computer Science, 1993.
- Lopez-Paz, D. et al. Gradient episodic memory for continual learning. In *Advances in Neural Information Processing Systems*, pp. 6467–6476, 2017.
- Mallya, A. and Lazebnik, S. Packnet: Adding multiple tasks to a single network by iterative pruning. In *Proceedings of the IEEE Conference on Computer Vision and Pattern Recognition*, pp. 7765–7773, 2018.
- Mariani, G., Scheidegger, F., Istrate, R., Bekas, C., and Malossi, C. Bagan: Data augmentation with balancing gan. *arXiv preprint arXiv:1803.09655*, 2018.
- Mnih, V., Kavukcuoglu, K., Silver, D., Graves, A., Antonoglou, I., Wierstra, D., and Riedmiller, M. Playing atari with deep reinforcement learning. *arXiv preprint arXiv:1312.5602*, 2013.
- Nguyen, C. V., Li, Y., Bui, T. D., and Turner, R. E. Variational continual learning. *arXiv preprint arXiv:1710.10628*, 2017.
- Rebuffi, S.-A., Kolesnikov, A., Sperl, G., and Lampert, C. H. icarl: Incremental classifier and representation learning. In *Proc. CVPR*, 2017.
- Ribando, J. M. Measuring solid angles beyond dimension three. *Discrete & Computational Geometry*, 36(3):479–487, 2006.
- Robins, A. Catastrophic forgetting, rehearsal and pseudorehearsal. *Connection Science*, 7(2):123–146, 1995.
- Rusu, A. A., Rabinowitz, N. C., Desjardins, G., Soyer, H., Kirkpatrick, J., Kavukcuoglu, K., Pascanu, R., and Hadsell, R. Progressive neural networks. *arXiv preprint arXiv:1606.04671*, 2016.
- Shin, H., Lee, J. K., Kim, J., and Kim, J. Continual learning with deep generative replay. In *Advances in Neural Information Processing Systems*, pp. 2990–2999, 2017.
- Vitter, J. S. Random sampling with a reservoir. *ACM Transactions on Mathematical Software (TOMS)*, 11(1): 37–57, 1985.
- Xu, J. and Zhu, Z. Reinforced continual learning. *arXiv preprint arXiv:1805.12369*, 2018.

Zenke, F., Poole, B., and Ganguli, S. Continual learning through synaptic intelligence. *arXiv preprint arXiv:1703.04200*, 2017.